Baryon Production at p-p Collider Experiments: Average p_t vs. Energy and Mass

Olga I. Piskounova

P.N.Lebedev Physics Institute of Russian Academy of Science, Leninski prosp. 53, 119991 Moscow, Russia

Abstract

This paper examines the transverse momentum spectra of baryons in the multi particle production at modern colliders using Quark-Gluon String Model (QGSM). It discusses 1) the difference in Λ^0 hyperon spectra at proton-antiproton vs. protonproton reactions; 2) the growth of average transverse momenta of Λ hyperon with proton-proton collision energies and 3) the dependence of average p_t on the masses of mesons and baryons at the LHC energy 7 TeV. This analysis of baryon spectra led to the following conclusions. First, the fragmentation of antidiquark-diquark side of pomeron diagram makes the major contribution to baryon production spectra in the asymmetric $p-\bar{p}$ reaction. Second, the average p_t 's of hyperons steadily grow with energy on the range from $\sqrt{s}=53$ GeV to 7 TeV. Since no dramatic changes were seen in the characteristics of baryon production, the hadroproduction processes do not cause the "knee" in the cosmic ray proton spectra at the energies between Tevatron and LHC. Third, the average transverse momentum analysis, through examining the different mass of hadrons, reveals the regularity in the mass gaps between baryon-meson generations. This observation gives the possibility for more hadron states with the masses: 13.7, 37.3, 101.5, 276, 750... GeV, which are produced by geometrical progression with the mass factor of order $\delta(\ln M)=1$. These hadrons may possess new quantum numbers or consist of heavy multi quarks.

1 Introduction

The aim of this paper is to analyze the transverse momentum spectra of hadrons from the modern collider experiments (ISR $^1, \rm STAR~^2, \rm UA5~^4,~UA1~^3,~CDF~^5,~AL-ICE~^6,~ATLAS~^7$ and CMS $^8)$. A number of reasons warrant this study. First of all, the preliminary compilation of data on Λ^0 hyperon transverse momentum distributions 2,4 demonstrates a difference in the dynamics of multi particle production in proton-proton vs. antiproton-proton collisions, which suggests that the baryon spectra are sensitive to the asymmetrical reactions where the fragmentation of diquark-antidiquark chain plays an important role. Secondly, the detailed study of characteristics of baryon spectra is necessary at the energies between Tevatron and LHC, because the cosmic ray proton spectrum has a "knee" in this range of energies 9 . The change in the slope of spectrum of protons, produced in the space, either have an astrophysical origin or can be explained by the substantial change in the dynamics of hadron production at this energy gap.

Finally, the course of average transverse momenta with the growth of hadron masses can demonstrate the availability of higher mass generations behind beauty hadrons, which supply the further increase of average transverse momenta. Interpretation of these distributions in the up-to-date phenomenological model can help resolve these issues.

The Quark-Gluon String Model [QGSM] approach is applied here to the description of p_t spectra for all available flavors of baryons 10,11 . The Model has

successfully described the large volume of data from previous generation of colliders up to the energies \sqrt{s} = 53 GeV in the area of low p_t 's ¹². Recently, Λ^0 hyperon production have been studied in updated version of QGSM ¹³.

The figure 1 presents the compilation of the data, $dN^{(\Lambda^0)}/dp_t$, in the region 0.1 GeV/c < p_t < 5 GeV/c from the following experiments (ISR ¹, STAR ², UA1 ³, UA5 ⁴ and CDF ⁵). It illustrates the changes in hyperon transverse distributions in the energy distance from ISR to Tevatron experiments. Since to calculate the average p_t we do not need only the absolute values of distributions, those are chosen arbitrarily. The range of low p_t 0.3 GeV/c < p_t < 4 GeV/c has the most impact on the value of average p_t . The figure clearly shows that average transverse momenta grow with energy.

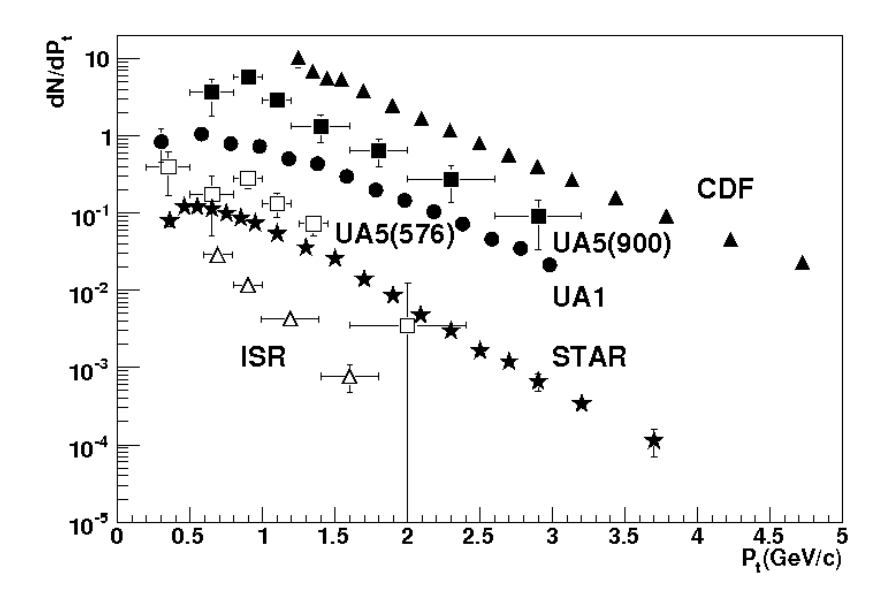


Figure 1: Transverse momentum distributions of Λ^0 hyperons from colliders that preceded LHC. The data are from ISR 1 p-p at $\sqrt{s}=53GeV$ - empty triangles, STAR 2 p-p at $\sqrt{s}=200$ GeV - black stars; UA5 $^4\bar{p}-p$ energies: 546 GeV(empty squares) and 900 GeV(black squares); UA1 3 $\bar{p}-p$ (630 GeV) - black circles and CDF 5 $\bar{p}-p$ at 1.8 TeV - black triangles.

2 Preliminary Comparison of Hyperon Transverse Momentum Spectra from LHC Experiments

The recent data on Λ^0 hyperon distributions are obtained in the following LHC groups: ALICE ⁶ at 900 GeV, ATLAS ⁷ and CMS ⁸ at 900 GeV and 7 TeV. We are going to compare the results of these LHC experiments with the data of lower energy p-p colliders, ISR $^1(\sqrt{s}=53GeV)$ and STAR $^2(\sqrt{s}=200GeV)$.

In the figure 2 the B values, the slopes of spectra, change, if we fit the data with a simple exponential function: $\exp(-B^*p_t)$.

We can conclude that transverse momentum spectra are harder with the energy growth that provides the change in the slopes, beginning from B=4,2 for ISR data, B=2,6 for STAR and to B=2,0 at 900 GeV in ALICE. The slope is flatter at \sqrt{s} = 7 TeV, B = 1,5. The calculation of average transverse momenta requires a detailed description of spectra, see section 3.

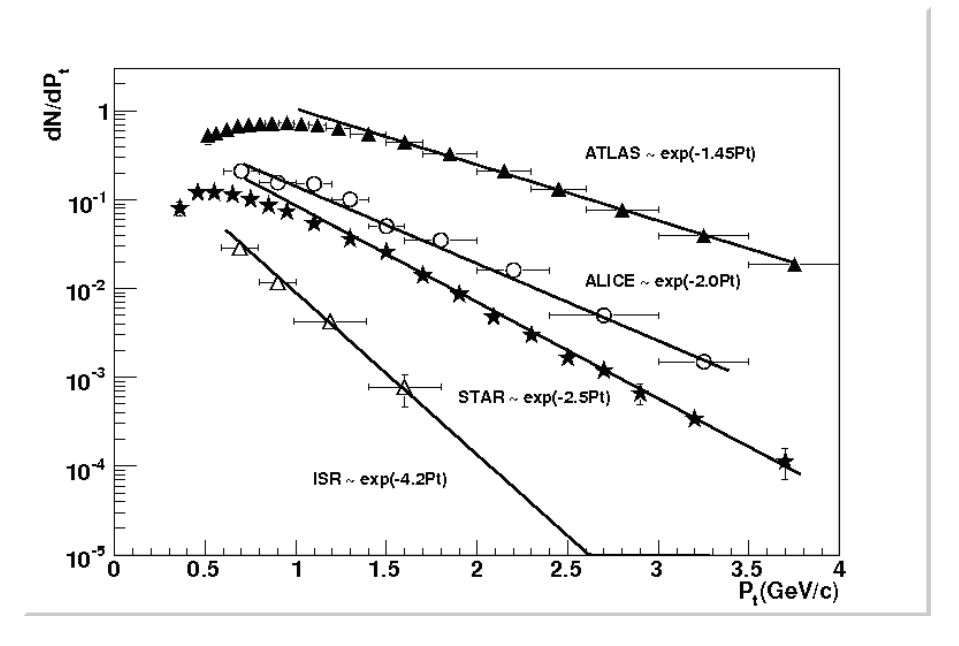


Figure 2: Transverse momentum distributions from p-p collider experiments: ISR¹ (53 GeV) - empty triangles, STAR² (200 GeV) - black stars, ALICE⁶ (900GeV) - empty circles and ATLAS⁷ (7 TeV) - black triangles, as fitted with the exponents.

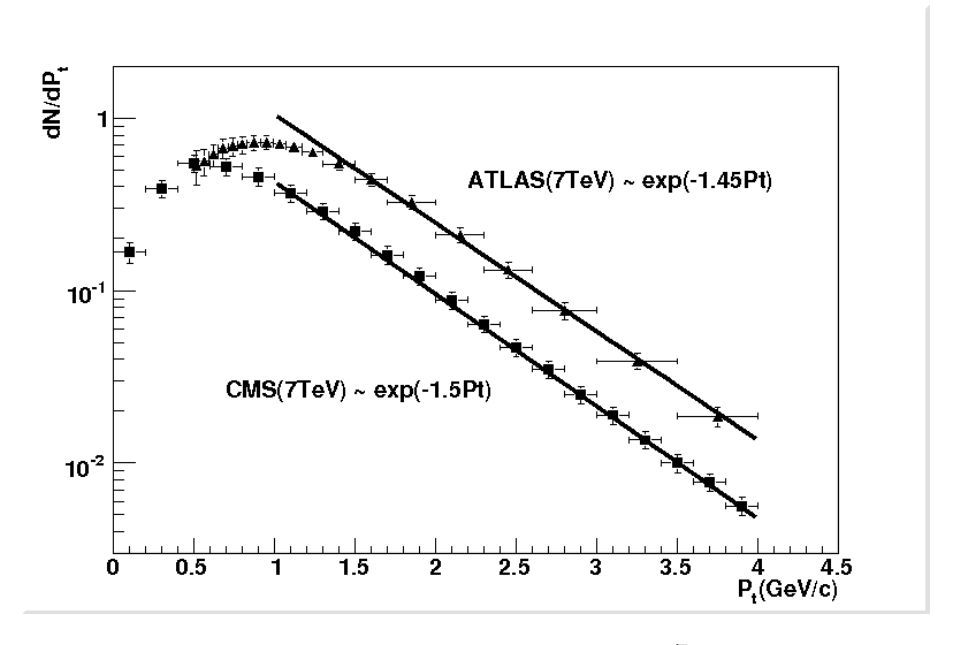


Figure 3: Transverse momentum distributions at \sqrt{s} = 7 TeV: ATLAS 7 - black triangles and CMS]citecms - black squares

Both LHC experiments at 7 TeV, ATLAS and CMS, have presented the hyperon spectra with the same slopes as expected (see the figure 3). The different forms of the distributions at low p_t region might be caused by efficiency specifics of ATLAS experiment.

3 Baryon Transverse Momentum Distributions in QGSM

The QGS Model has been devised for the description of rapidity distributions and hadron spectra in x_F^{10} . The Model operates with pomeron diagrams (see the figure 6), which help calculate the rapidity spectra. These spectra are presented as the convolutions of constituent quark structure functions with the diquark-antidiquark pair distributions at the pomeron cylinder fragmentation into baryons. This approach took into account mostly the average p_t values for given energy. The early QGSM study 12 on the hadron transverse momentum distributions has shown that the spectra of baryons in proton-proton collisions can be described with the following p_t -dependence:

$$E\frac{d^{3}\sigma^{H}}{dx_{F}d^{2}p_{t}} = \frac{d\sigma^{H}}{dx_{F}} * A_{0} * \exp[-B_{0} * (m_{t} - m_{0})], \tag{1}$$

where m_0 is the mass of produced hadron, $m_t = \sqrt{p_t^2 + m_0^2}$. The slope parameter, B_0 , used to bring the dependence on x_F in previous research ¹². The values of B_0 for the spectra of many types of hadrons (π, K, p) were estimated for the data of proton-proton collisions up to the energies of ISR experiment. The value of the slopes of baryon spectra for the data in central region of rapidities was universal and equal to $B_0 = 6,0$.

As discussed above, the slopes of spectra, B_0 , at the modern collider experiments depend on energy. Moreover, the form of spectra at LHC and RHIC indicates that the value of m_0 is not the mass of proton or hyperon. A better description of hyperon spectra can be achieved with $m_0 = 0.5$ GeV that is actually the mass of kaon, see the figure 4. This effect can be provisionally explained as the minimal transverse momentum of hyperon at the fragmentation of diquark-quark chain (see the QGSM pomeron diagram for p-p collisions in the figure 6). The value of m_0 should be equal to the kaon mass, because the minimal diquark-quark chain fragmentation produces only two hadrons: Λ^0+K .

4 The Difference between Distributions in Proton-Proton and Antiproton-Proton Collisions

Here we consider the difference in the spectra of baryon production in symmetric (p-p) and asymmetric $(\bar{p}-p)$ reactions.

4.1 The Data of UA5 Experiment

This subsection discusses the influence of quark composition of beam particles on the shape of transverse momentum spectra of Λ^0 hyperon production. The data from p- \bar{p} experiments UA5 4 of energies, \sqrt{s} = 200 GeV and 546 GeV, are studied (see figure 5).

The sharp exponential contribution to spectra is seen in $\bar{p} - p$ reaction at $\sqrt{s} = 546$ GeV in UA5 collaboration data⁴ at very low $p_t < 0.5$ GeV/c, see the figure 5.

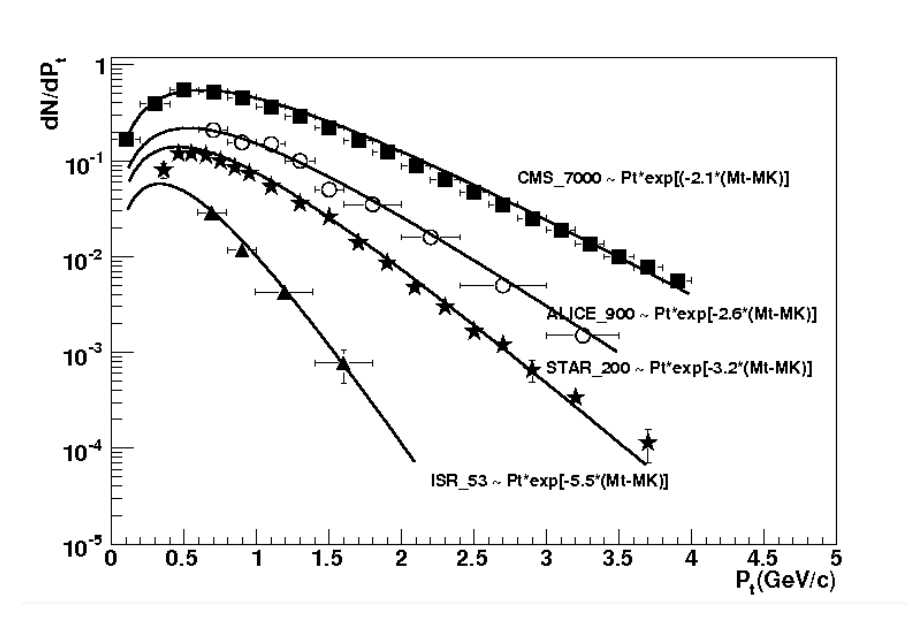


Figure 4: The description of proton-proton experiment data ISR^1 (53 GeV), $STAR^2$ (200 GeV), ALICE 6 (900GeV) and CMS 8 (7 TeV) data on hyperon production with the QGSM fit.

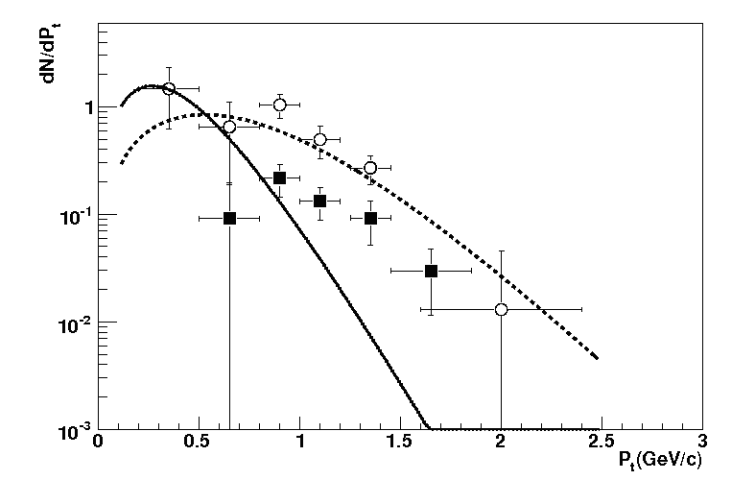


Figure 5: The forms of spectra at antiproton-proton reaction in $UA5^4$ - black squares at the energy \sqrt{s} =200 GeV. The $UA5^4$ data of higher energy (\sqrt{s} =546 GeV) are shown with empty squares. As I mentioned above, the absolute values of spectra are chosen arbitrarily. The fit for UA5(546) with solid and dashed lines demonstrates two different components at the asymmetric one-pomeron cut.

This exponential component might exist in other antiproton-reaction spectra as well, but it is not seen because of the absence of measurements in low p_t 's.

The form of the spectrum at low p_t has a strong impact on the value of cross section, if the experimental distributions are integrated beginning from low momenta, $p_t = 0.3 \text{ GeV/c}$. The resulting cross section from antiproton-proton reaction should be smaller than the cross section, obtained in proto-proton collision of the same energy, if there are no data points at $p_t < 0.5 \text{ GeV/c}$. The complex form of spectra in UA5 can be explained by two component spectra for antiproton-proton collisions. The QGSM diagrams explain the nature of two components in the asymmetrical reaction.

4.2 The Difference in Distributions from antiproton-proton and proton-proton reactions in QGSM

The difference in p_t -spectra of Λ^0 's produced in high energy p-p and $\bar{p}-p$ collisions cannot be explained in the perturbative QCD models, since both interactions should give the mutiparticle production in central rapidity region due to dominating one Pomeron exchange. The total cross section and the spectra in p-p and $\bar{p}-p$ collisions should be equal because they depend only on the parameters of the Pomeron exchange between two interacting hadrons and should not be sensitive to the quark contents of colliding particles.

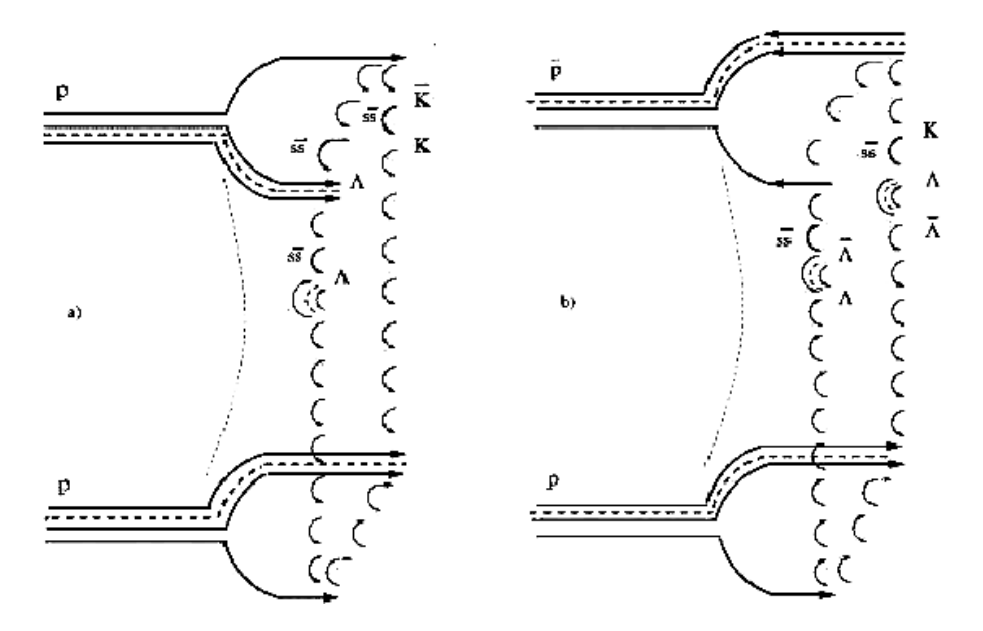


Figure 6: QGSM multiparticle production diagrams for a) proton-proton and b) antiproton-proton reactions.

The pomeron diagrams of p-p and $\bar{p}-p$ collisions are shown in the figure 6. In the framework of QGSM 10,11 , which is based on the Regge theory and on the phenomenology of pomeron exchange, the spectra of produced particles are the results of the cut of one-pomeron diagrams. The comparison of diagrams shows that the most important contribution to hadron production spectra in $\bar{p}-p$ reaction is brought by the fragmentation of antidiquark-diquark chain of pomeron cylinder, because this side of diagram takes the greater part of energy of colliding particles. Otherwise, the p-p collision diagram is symmetric and built from two similar quark-diquark chains. Therefore, the incorrect description of the region of small

transverse momenta at antiproton-proton reaction leads to underestimated values of cross section. The figure 7 shows that baryon production at low energy goes with the quark-antiquark annihilation. The resulting spectra consist of the contribution from only diquark-antidiquark chain that allows us to see the pure form of baryon transverse momentum distributions in asymmetric case of fragmentation. The form of baryon spectra in antiproton-proton reaction of low energy was planned to be studied in experiment TAPAS ¹⁴.

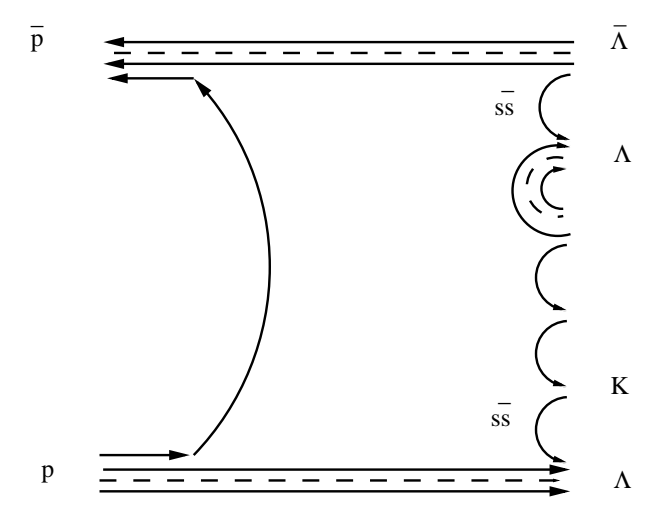


Figure 7: The low energy diagram with quark-antiquark annihilation and diquark-antidiquark chain fragmentation.

Since LHC collider has proton projectiles, the transverse momentum distribution of hyperon production seems "softer" in comparison to the Monte Carlo (MC) generator predictions ¹⁵ that were preliminary tuned to the Tevatron data.

5 Average Baryon Transverse Momenta vs. Energy and "Knee" in Cosmic Ray Spectra

As the data on baryon distributions in antiproton-proton reactions are irrelevant for consideration, the spectra from LHC can be compared only with measurements of proton-proton collision experiments: ISR and STAR. We consider the transverse momentum spectra in the wide range of energies: beginning from 53 GeV to the LHC energy 7 TeV.

The cosmic ray proton spectrum shows the "knee" (see figure 8) at the energy gap between Tevatron and LHC colliders ⁹. The change in the slope of proton spectrum at $E_{lab} \approx 3*~10^{15}$ eV might be a manifestation of a new regime in hadronic interactions. Otherwise, the change in the spectrum may have an astrophysical origin. The analysis of average baryon transverse momenta in the framework of QGSM clearly demonstrates that the average transverse momentum of baryons grows steadily with energy (see figure 9).

The $\langle p_t \rangle$ values grow in the range of energy from 53 GeV (ISR) up to \sqrt{s} = 200 GeV (STAR) and then they go with the asymptote $s^{0.05}$. This behavior cannot be considered as substantial change in hadroproduction processes. Since no spesific points exist in baryon production up to $\sqrt{s} = 7$ TeV, which corresponds to $E_{lab} = 2.5 * 10^{16}$ eV, it is reasonable to conclude that "knee" has an astrophysical

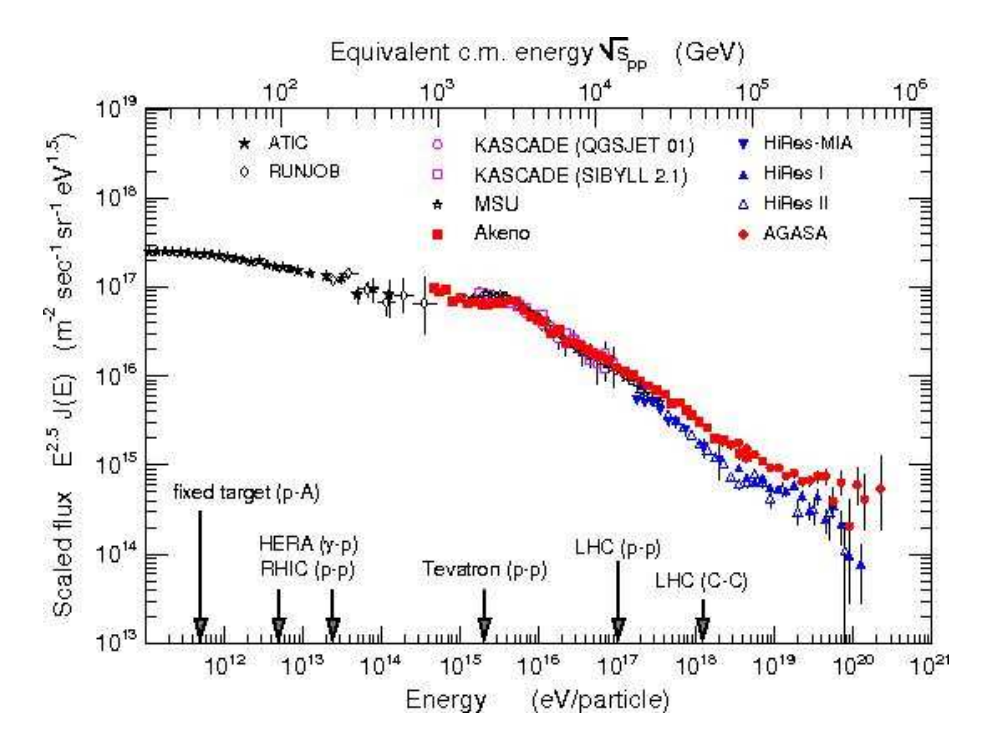


Figure 8: The cosmic proton spectrum with the "knee" between Tevatron and LHC energies.

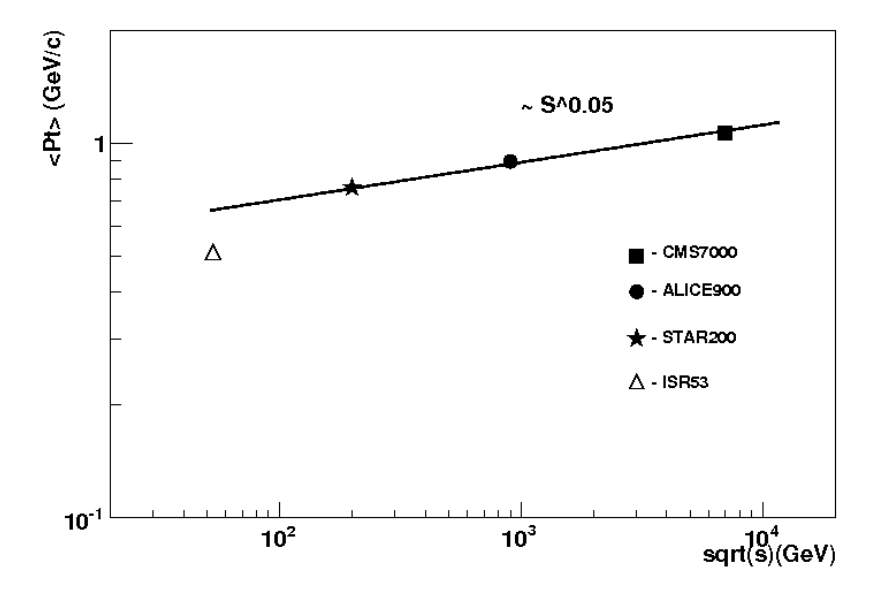


Figure 9: Average transverse momenta of hyperons increase with the energy, as $s^{0.05}$.

explanation. For instance, the "knee" may indicate the maximal energy of protons that are produced in a nearest galaxy.

The growth of average transverse momenta was calculated in the framework of QGSM on the energy distance up to LHC. This result should be used for the interpretation of futher data of LHC groups. However, the energy dependence of $\langle p_t \rangle$ is not yet included into MC generators calculations. In such a way, the results of this research will help improve LUND, Pythia and other MC models.

6 Average Transverse Momenta vs. Mass of Hadrons

The previously published analysis of transverse momentum spectra of baryons from LHC experiments (ALICE, ATLAS, CMS)¹⁶ provided only partial data on hadron spectra. In order to get a full understanding of average transverse dependence on hadron mass, we supplement here the data with the spectra of kaons, D-mesons and B-mesons from LHC ¹⁷ at 7 TeV. The heavy quark meson spectra were fitted with the same formula (1) as the baryon spectra (see the figure 10).

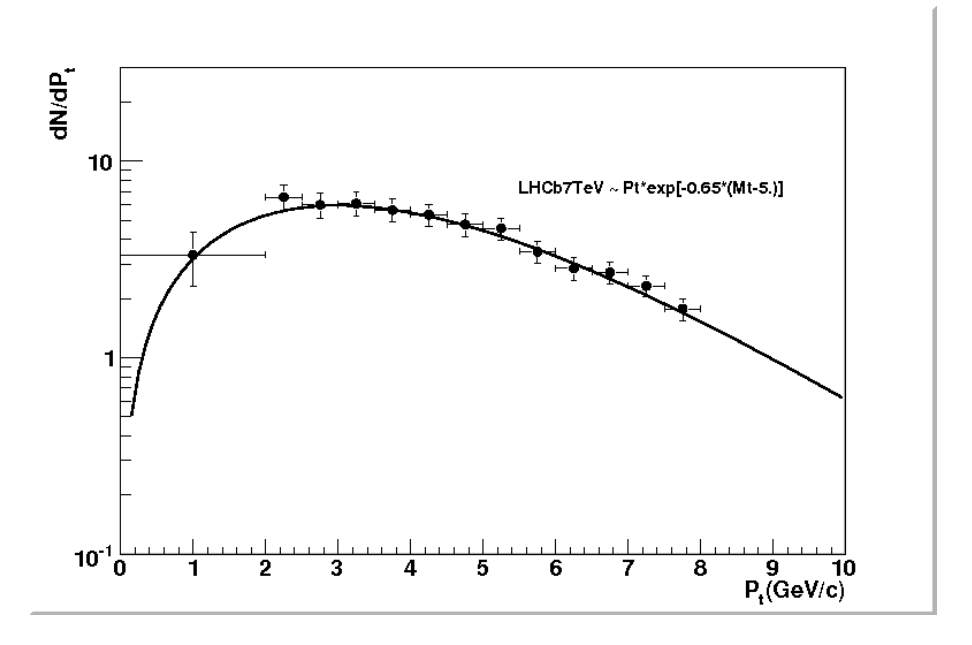


Figure 10: The QGSM fit of B-meson spectra at \sqrt{s} =7 TeV in LHCb¹⁷ experiment.

As the result of the fit, the average p_t of B-mesons is equal to 4,46 GeV at the energy $\sqrt(s)$ =7 TeV. The dependence of average transverse momenta on the mass of hadron in the figure 11 shows that $< p_t >$'s grow with masses. If we imagine symmetric point between meson and baryon masses of a given quark flavor, the mass distance between points of one hadron generation and the next one can be estimated with the mass factor $\delta lnM_H = 1$. It means that we have the geometric progression for the masses of hypotetical hadrons.

The extension of this sequence provides the hadron states with the following masses: 13.7, 37.3, 101.5, 276, 750 GeV and so forth. The plot is expanded with average p_t dependence $\langle p_t \rangle \propto M_H^{0.1}$ above the bottom hadron masses. These hypothetical hadrons bring new quantum numbers or represent heavy multi quark states. This hypothesis attempts to predict new particles and helps achieve the unification of baryon and meson features at heavy masses revisited recently in ¹⁹. It

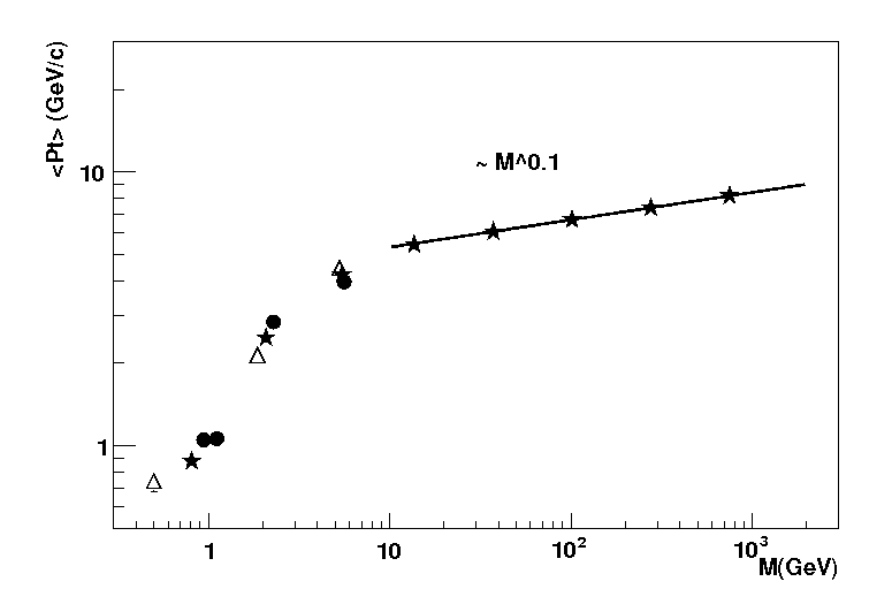


Figure 11: The mass dependence of average momenta of hadrons (mesons - empty triangles, baryons - black circles). The extensions for the hypothetical heavy hadron states are shown with the black stars.

should be noted, however, that the mass of top quark does not match the suggested collection of new hadron states, which warrants further research.

7 Conclusions

The overview of results in transverse momentum distributions of hyperons produced in proton-proton collisions of various energies ^{13,22} has revealed a significant change in the slopes of baryon spectra in the region of $p_t = 0.3$ - 8 GeV/c. The spectra of baryons become harder with the energy growth from ISR(\sqrt{s} =53 GeV) and RHIC (200 GeV) up to LHC (0,9 and 7 TeV). The detailed analysis of hyperon spectra in the framework of QGSM demonstrates the change of slopes from $B_0 = 4.6$ (ISR at 53 GeV) to $B_0 = 2.1$ (LHC at 7 TeV). The transverse momentum baryon spectra in antiproton-proton collisions (UA1, UA5, CDF) differ from the p_t distributions of baryons in proton-proton collisions (ISR, STAR, LHC). QGSM explains this phenomenon as a difference in the splitting of transverse energy between two sides of pomeron diagram. The cut diagram for antiproton-proton case includes the unusual side with the diquark-antidiquark ends, which accumulates more energy than another quark-antiquark side of cylinder. It is reasonable to suggest that the difference in spectra disappears with the growth of energy due to the increasing multipomeron contributions into the differential cross section that are similar for both $\bar{p}-p$ and p-p collisions. The average p_t values in proton-proton collisions grow steadily as the power of energy, $s^{0.05}$, up to highest LHC energy 7 TeV. Therefore, the baryon production processes at the energies of LHC are not totally random. This conclusion has crucial implications for cosmic ray physics, since it suggests that the "knee" at $E_{lab} \approx 4^* \ 10^{15}$ eV in cosmic proton spectra does not originate in hadronic interactions. There is no significant change in baryon spectra up to \sqrt{s} = 7 TeV corresponding to $E_{lab} = 2.5 * 10^{16}$ eV in the cosmic ray physics. I suggest that the "knee" may indicate the maximal energy of protons from a nearest galaxy. The idea of proton production in space warrants a further detailed investigation of the hadroproduction dynamics in the framework of QGSM.

The average transverse momentum analysis, through examining the different mass of hadrons, indicates a regularity in the mass gaps between heavy quark baryon-meson generations. This observation gives the possibility for more hadron states with the masses: 13.7, 37.3, 101.5, 276, 750... GeV, which are produced by geometrical progression with the mass multiplier of order $\delta(\ln M)=1$. These hadron states may possess new quantum numbers or consist of heavy multi quarks. Since the results of this research shed new light on baryon production at LHC, they should be considered in current MC generators, as LUND, Pythia etc. This study shows that the results of phenomenological analysis of experimental data have far-reaching implications for the high energy physics.

8 Acknowledgments

I would like to thank the Russian Foundation of Fundamental Research (grant 13-02-06091) and Dmitry Zimin's "Dynasty" Foundation. Their financial supports made possible the First Kaidalov's Phenomenology Workshop. This workshop has given the boost to the phenomenological research that is described in my paper.

9 References

- 1. ISR Collaboration, D.Drijard et al. Z.Phys. C12, 217,1982.
- 2. STAR Collaboration, B.I. Abelev et al, Phys. Rev. C75, 064901,2007.
- 3. UA1 Collaboration, G. Bocquet et al, Z. Phys. C366,441,1996.
- 4. UA5 Collaboration, R.E. Ansorge et al, Nucl. Phys.B328,36,1989.
- 5. CDF Collaboration, D. Acosta et al, Phys. Rev. D72, 052001,2005.
- 6. ALICE Collaboration, EPJ C71,1594,2011, e-print arXiv:1012.3257.
- 7. ATLAS Collaboration, Aad et al, PR D85,012001, e-print arXiv:1111.1297.
- 8. CMS Collaboration, Khachatryan *et al*, JHEP 05,064, e-print arXiv:1102.4282.
- 9. V. B. Petkov, O. D.Lalakulich, G. M.Vereshkov, Phys.Atom.Nucl.66,523, 2003; Jorg R. Horandel, N.N.Kalmykov, A.V.Timokhin, Jou.of Phys.: Conference Series 47 (2006) 132.
- Quark-Gluon String Model, A.B. Kaidalov and K.A. Ter-Martirosyan, Sov.J.Nucl.Phys.39, 1545, 1984, 40, 211, 1984, A.B. Kaidalov, Phys.Lett.B116, 459, 1982.
- A.B. Kaidalov and O.I. Piskunova Z. Phys. C30,145,1986, O.I. Piskounova Nucl. Phys. Proc. Suppl. 93, 144, 2001, e-Print: hep-ph/0010263.
- A.I. Veselov, O.I. Piskunova, K.A. Ter-Martirosian, Phys.Lett.B158, 175, 1985.
- O.I. Piskounova, e-Prints arXiv:1101.1852, 1209.6214, 1301.6539 and later G.H. Arakelyan, C. Merino , Yu. M. Shabelski, Phys.Atom.Nucl. 77 (2014) 626.
- 14. Giorgio Apollinari (Fermilab), Olga Piskunova et al., FERMILAB-TAPAS-PROPOSAL-1022, Fermilab, 2011.
- B. Alessandro et al. Hadron-Hadron and Cosmic-Ray Interactions at multi-TeV Energies workshop, Trento, Italy, 29 Nov - 3 Dec 2010 Proceedings, e-Print arXiv:1101.1852.
- 16. A.A. Bylinkin(Moscow, MIPT) and O.I.Piskounova (LPI), Nucl.Part.Phys.Proc. 273-275 (2016) 2752, e-Print arXiv:1501.07706.

- 17. LHCb Collaboration, JHEP **04**(2012)93, e-print arXiv:1202.4812.
- 18. Y.R. de Boer (Twente Uni.), A.B. Kaidalov (ITEP), D.A.Milstead (Stockholm Uni.) and O.I. Piskounova (LPI), J.Phys. G35(2008)075009, e-Print arXiv 0710.3830.
- 19. Stanley J. Brodsky et al, Int.J.Mod.Phys. A **31**(2016)1630029.
- 20. LHCb Collaboration, Chin.Phys.C,C40(2016)011001, e-Print arXiv:1509.00292.
- 21. O.I.Piskounova, Phys.Atom.Nucl.**64**(2001) 392, e-Print: hep-ph/0001252.
- 22. Olga Piskounova, in the Proceedings of "38th International Conference of High Energy" PoS(ICHEP2016)711, e-print arXiv:1706.07648.